GAUGE-VARIANT PROPAGATORS AND THE RUNNING COUPLING FROM LATTICE QCD

E.-M. ILGENFRITZ, M. MÜLLER-PREUSSKER, A. STERNBECK
Humboldt-Universität zu Berlin, Institut für Physik, Newtonstr. 15, D-12489 Berlin, Germany

A. SCHILLER
Universität Leipzig, Institut für Theoretische Physik, Vor dem Hospitaltore 1, D-04103 Leipzig, Germany

On the occasion of the 70's birthday of Prof. Adriano Di Giacomo we report on recent numerical computations of the Landau gauge gluon and ghost propagators as well as of a non-symmetric MOM-scheme ghost-gluon vertex in quenched and full lattice QCD. Special emphasis is paid to the Gribov copy problem and to the unquenching effect. The corresponding running coupling $\alpha_s(q^2)$ is found and shown to decrease for $q^2 \leq 0.3$ GeV^2 in the infrared limit. No indication for a non-trivial infrared fixed point is seen in agreement with findings from truncated systems of Dyson-Schwinger equations treated on a four-dimensional torus.

1 Introduction

Three of us (E.-M.I., M.M.-P. and A.S.) had the occasion to meet Adriano Di Giacomo many times since the late eighties. Over the years we shared with him the scientific interest on topological aspects in connection with the confinement property of Yang-Mills theories. For us it was always helpful and exciting to listen to and to discuss with him and to follow his ideas and his opinion. We would like to wish him all the best and to be continuously active in science in the future.

In our contribution to this honorary collection of papers we would like to report on a field theoretic investigation closely related to the confinement problem which became popular over the last decade. It considers the infrared behaviour of the Landau gauge gluon and ghost propagators in QCD in connection with the Gribov-Zwanziger horizon condition[1,2] and the Kugo-Ojima criterion[3]. The propagators also provide a nonperturbative determination of the running QCD coupling $\alpha_s(q^2)$ in a MOM scheme. It is a great advantage to be able to compute the relevant Green functions within the framework of truncated systems of Dyson-Schwinger (DS) equations as well as within the lattice approach and to check the consistency of both approaches. As we shall discuss below, for the infinite volume case there is still a mismatch between the infrared limit results, what requires further investigations in the near future.

In the infinite 4-volume limit the DS approach has led to an intertwined infrared power behaviour of the gluon and ghost dressing functions[4,5,6,7,8]

$$\begin{aligned} Z_D(q^2) &\equiv q^2 D(q^2) \propto (q^2)^{2\lambda}\,, \\ Z_G(q^2) &\equiv q^2 G(q^2) \propto (q^2)^{-\lambda} \end{aligned} \tag{1}$$

with the same $\lambda \approx 0.59$, *i.e.* a vanishing gluon propagator $D(q^2)$ in the infrared occurs in intimate connection with a diverging ghost propagator $G(q^2)$. Under the condition that the ghost-gluon vertex renormalization function $Z_1(\mu^2)$ is finite and constant (see[9]

for the perturbative proof and [10] for a first $SU(2)$ lattice study) the corresponding MOM scheme running coupling is determined by

$$\alpha_s(q^2) = \frac{g^2}{4\pi}\, Z_D(q^2)\, Z_G^2(q^2)\,. \tag{2}$$

This means that Eq. (1) leads to a non-trivial fixed point of α_s in the infrared limit [8]. As we shall show below, our lattice simulations do not agree with this prediction. The strong coupling $\alpha_s(q^2)$ seems to tend to zero in this limit as lattice results for other definitions of the running coupling also indicate (see [11,12] for the three-gluon vertex and [13] for the quark-gluon vertex).

Possible solutions of the discrepancy have been discussed from different points of view in the recent literature. In [14,15] the DS approach has been studied on a finite 4-torus with the same truncated set of equations as for the infinite volume. $\alpha_s(q^2)$ was shown to tend to zero for $q^2 \to 0$ in one-to-one correspondence with what one finds on the lattice. This would indicate very strong finite-size effects and a slow convergence to the infinite-volume limit. However, on the lattice we do not find any indication for such a strong finite-size effect, except the convergence to the infinite-volume limit would be extremely slow. An alternative resolution of the problem has been proposed by Boucaud *et al.* [16]. These authors argued the ghost-gluon vertex in the infrared might contain q^2-dependent contributions which could modify the DS results for the mentioned propagators [a]. However, recent detailed DS studies of the ghost-gluon vertex did not provide hints for such a modification [17,18]. Thus, at present there seems to be no solution of the puzzle.

For $SU(2)$ extensive lattice investigations can be found in [19]. Unfortunately, the authors did not reach the interesting infrared region, where the mentioned inconsistencies become visible. The same holds for previous $SU(3)$ lattice computations of the ghost and gluon propagators as reported in [20,21,22]. We have been pursuing an analogous study for the $SU(3)$ case with special emphasis on the Gribov copy problem [23]. Moreover, we have investigated the spectral properties of the Faddeev-Popov operator [24]. The low-lying eigenmodes of the latter are expected to be intimately related to a diverging ghost propagator. In addition, in [25] we have reported on a first $SU(3)$ lattice computation of the ghost-gluon vertex at zero gluon momentum. We confirm, what has been found already for $SU(2)$, namely that the data are quite consistent with a constant vertex function [10].

For the given report we have extended our investigations restricted so far to pure $SU(3)$ Yang-Mills theory to the full QCD case with $N_f = 2$ clover-improved Wilson fermions. For the latter case we have used lattice field configurations produced by the QCDSF collaboration and made available via the International Lattice DataGrid (ILDG)[b].

2 Landau gauge fixing, lattice gluon and ghost propagators

As a first step we have studied the gluon and ghost propagators in the quenched approximation. $SU(3)$ gauge field configurations $U = \{U_{x,\mu}\}$ thermalized with the standard

[a] We thank A. Lokhov for bringing us the arguments in [16] to our attention.

[b] We thank Gerrit Schierholz and the QCDSF members for giving us access to their configurations.

Wilson gauge action have been put into the Landau gauge by iteratively maximizing the gauge functional

$$F_U[g] = \frac{1}{4V} \sum_x \sum_{\mu=1}^{4} \mathrm{Re}\,\mathrm{Tr}\, {}^gU_{x,\mu}\,, \qquad {}^gU_{x,\mu} = g_x\, U_{x,\mu}\, g^\dagger_{x+\hat{\mu}} \tag{3}$$

with $g_x \in SU(3)$. It has numerous local maxima (Gribov copies), each satisfying the lattice Landau gauge condition

$$(\partial_\mu {}^gA_\mu)(x) \equiv {}^gA_\mu(x+\hat{\mu}/2) - {}^gA_\mu(x-\hat{\mu}/2) = 0 \tag{4}$$

for the gauge transformed lattice potential

$${}^gA_\mu(x+\hat{\mu}/2) = \frac{1}{2i}\left({}^gU_{x,\mu} - {}^gU^\dagger_{x,\mu}\right)\Big|_{\mathrm{traceless}}. \tag{5}$$

To explore to what extent this ambiguity has a significant influence on gauge dependent observables, we have gauge-fixed each thermalized configuration a certain number of times (several tens depending on lattice size and coupling) mostly using the *over-relaxation* algorithm, starting from random gauge copies. For each configuration U, we have selected the first (`fc`) and the best (`bc`) gauge copy (that with the largest functional value) for subsequent measurements. We have checked that for the `bc` copy the number of trials was sufficient for a convergence of the ghost propagator within the statistical noise. For details we refer to[23].

It turned out that the Gribov ambiguity has no systematic influence on the infrared behaviour of the gluon propagator. This holds as long as one restricts to periodic gauge transformations on the four-torus. In[26] the gauge orbits have been extended to the full gauge symmetry including also non-periodic $\mathbf{Z}(N)$ transformations. As a consequence the Gribov problem appears to be enhanced even for the gluon propagator. Here we restrict ourselves to the standard case of periodic gauge transformations. In marked contrast to the weak Gribov copy dependence of the gluon propagator the ghost propagator at lower momenta depends on the selection of gauge copies. (For a study of the influence of Gribov copies on the ghost propagator in the $SU(2)$ case see[27].)

The gluon propagator $D^{ab}_{\mu\nu}(q^2)$ is the Fourier transform of the gluon two-point function, *i.e.* the colour-diagonal expectation value

$$\begin{aligned} D^{ab}_{\mu\nu}(q) &= \left\langle \widetilde{A}^a_\mu(k)\widetilde{A}^b_\nu(-k)\right\rangle \\ &= \delta^{ab}\left(\delta_{\mu\nu} - \frac{q_\mu\, q_\nu}{q^2}\right) D(q^2)\,, \end{aligned} \tag{6}$$

where $\widetilde{A}^a_\mu(k)$ denotes the Fourier transform of $A^a_\mu(x+\hat{\mu}/2)$ and q is the physical momentum

$$q_\mu(k_\mu) = \frac{2}{a}\sin\left(\frac{\pi k_\mu}{L_\mu}\right) \tag{7}$$

related to the integer-valued lattice momentum $k_\mu \in (-L_\mu/2, L_\mu/2\,]$ for the linear lattice extension $L_\mu, \mu = 1,\ldots,4$. According to Ref.[28], a subset of possible lattice momenta k has been chosen for the final analysis of the gluon propagator, although the Fast

Fourier Transform algorithm provides us with all lattice momenta. In what follows for the quenched case we use the lattice spacing a in physical units as determined in[29].

The ghost propagator is derived from the Faddeev-Popov (F-P) operator, the Hessian of the gauge functional given in Eq. (3). We expect that the properties of the F-P operator differ for the different maxima of the functional (Gribov copies). This has consequences for the ghost propagator as is shown below. The F-P operator can be written in terms of the (gauge-fixed) link variables $U_{x,\mu}$ as

$$M^{ab}_{xy} = \sum_{\mu} A^{ab}_{x,\mu}\,\delta_{x,y} - B^{ab}_{x,\mu}\,\delta_{x+\hat{\mu},y} - C^{ab}_{x,\mu}\,\delta_{x-\hat{\mu},y} \tag{8}$$

with

$$\begin{aligned} A^{ab}_{x,\mu} &= \mathrm{Re\,Tr}\left[\{T^a,T^b\}(U_{x,\mu}+U_{x-\hat{\mu},\mu})\right], \\ B^{ab}_{x,\mu} &= 2\cdot\mathrm{Re\,Tr}\left[T^bT^a\,U_{x,\mu}\right], \\ C^{ab}_{x,\mu} &= 2\cdot\mathrm{Re\,Tr}\left[T^aT^b\,U_{x-\hat{\mu},\mu}\right] \end{aligned}$$

and T^a, $a=1,\ldots,8$ being the (hermitian) generators of the $\mathfrak{su}(3)$ Lie algebra satisfying $\mathrm{Tr}\,[T^aT^b] = \delta^{ab}/2$. The ghost propagator is then determined by inverting the F-P operator M

$$\begin{aligned} G^{ab}(q) &= \frac{1}{V}\sum_{x,y}\left\langle \mathrm{e}^{-2\pi i\,k\cdot(x-y)}[M^{-1}]^{ab}_{xy}\right\rangle_U, \\ &= \delta^{ab}G(q^2)\,. \end{aligned} \tag{9}$$

Following Ref.[20,30] we have used the conjugate gradient (CG) algorithm to invert M on a plane wave $\vec{\psi}_c$ with colour and position components $\psi^a_c(x) = \delta^{ac}\exp(2\pi i\,k\cdot x)$. In fact, we applied the pre-conditioned CG algorithm (PCG) to solve $M^{ab}_{xy}\phi^b(y) = \psi^a_c(x)$. As the pre-conditioning matrix we used the inverse Laplacian operator Δ^{-1} with diagonal colour substructure. This has significantly reduced the required amount of computing time (for details see [23]). After solving $M\vec{\phi} = \vec{\psi}_c$ the resulting vector $\vec{\phi}$ is projected back on $\vec{\psi}_c$ such that the average $G^{cc}(q)$ over the colour index c (divided by V) can be taken explicitly. Since the F-P operator M is singular if acting on constant modes, only $k \neq (0,0,0,0)$ is permitted. Due to high computational requirements to invert the F-P operator for each k, separately, the estimator on a single, gauge-fixed configuration is evaluated only for a preselected set of momenta k.

3 Quenched QCD results

In Fig. 1 we show the ghost and the gluon dressing functions $Z_{G,D}(q^2)$ versus q^2 for `fc` copies in the present state of our quenched QCD simulations. Both propagators have been renormalized separately for each β with the normalization condition $Z_{G,D} = 1$ at $q = 4$ GeV.

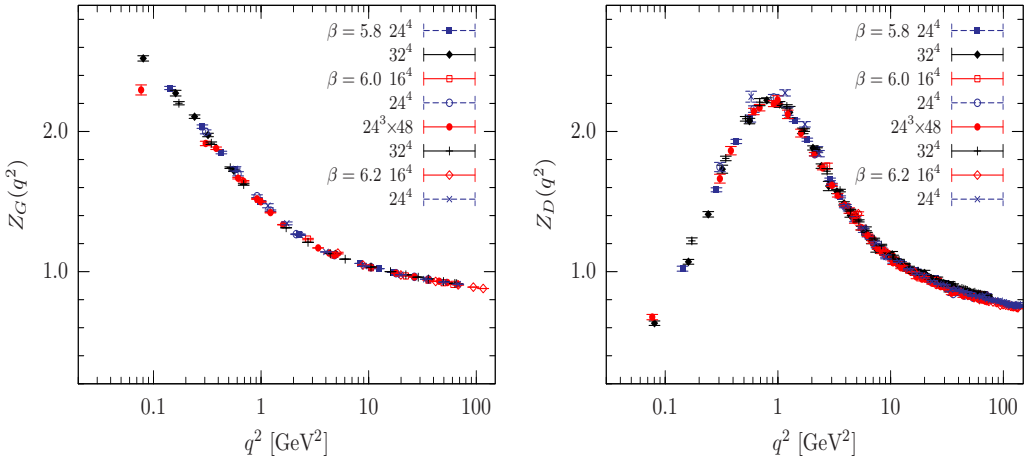

Figure 1: The dressing functions for the ghost $Z_G \equiv q^2 G(q^2)$ (l.h.s.) and gluon propagator $Z_D \equiv q^2 D(q^2)$ (r.h.s.) vs. q^2 for quenched QCD, both measured on `fc` gauge copies.

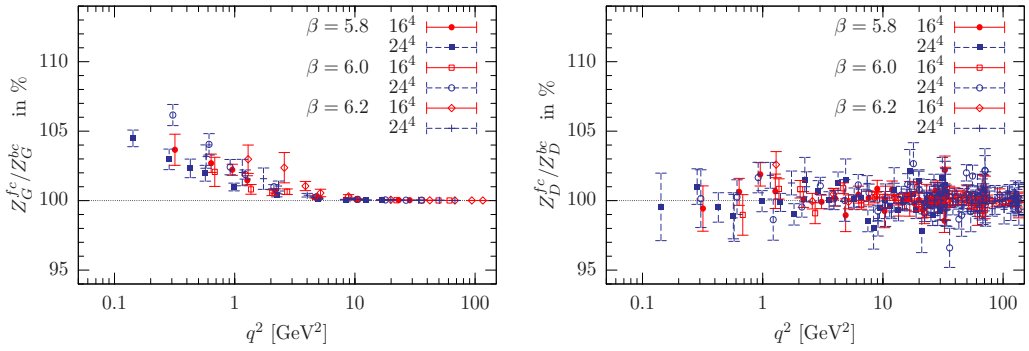

Figure 2: The ratios $Z^{\rm fc}/Z^{\rm bc}$ for the dressing functions Z_G (l.h.s.) and Z_D (r.h.s.) determined on first (`fc`) and best (`bc`) gauge copies *vs.* momentum q^2.

In Fig. 2 we illustrate the effect of the Gribov copies for periodic gauge transformations. We have plotted some `fc` - to - `bc` ratios of the ghost and gluon dressing functions. Obviously there is no influence visible for the gluon propagator within the statistical noise. On the contrary, for the ghost propagator the Gribov problem can cause $O(5\%)$ deviations in the low-momentum region ($q < 1$ GeV). For better gauge copies the ghost dressing function becomes less singular in the infrared. A closer inspection of the data for the ghost propagator indicates that the influence of Gribov copies becomes weaker for **increasing** lattice size. This is in agreement with a recent claim by Zwanziger according to which in the infinite volume limit averaging over gauge copies in the Gribov region should lead to the same result as averaging over copies restricted to the fundamental modular region[31]. In[26] similar indications have been found for $SU(2)$ taking non-periodic $Z(2)$ transformations into account.

Note in Fig. 1 the deviation of the lowest-momentum Z_G data point obtained on an asymmetric lattice $24^3 \times 48$. This deviation deserves further study and sheds some critical

light on investigations on strongly asymmetric lattices[32,33]. Still it remains difficult to extract a possible power behaviour at low q^2 as in Eq. (1).

In Fig. 3 we present the combined result for the running coupling according to Eq. (2) for `fc` copies in the quenched QCD case. Fits to the 1-loop and 2-loop running coupling are also shown. Our data confirm the running coupling monotonously to decrease with

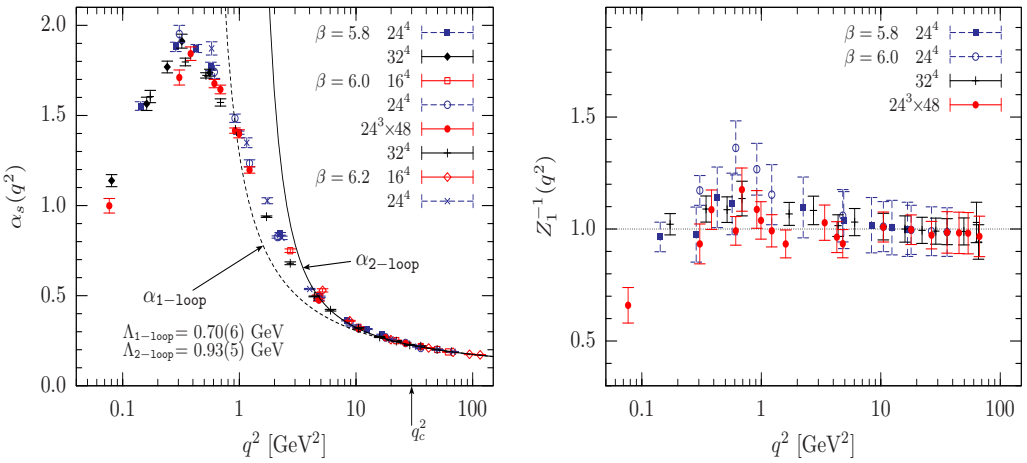

Figure 3: L.h.s.: The momentum dependence of the running coupling $\alpha_s(q^2)$ for quenched QCD measured on `fc` gauge copies. R.h.s.: The inverse ghost-gluon vertex renormalization function $Z_1^{-1}(q^2)$ measured on `fc` gauge copies and normalized to unity at $q = 4$ GeV.

decreasing momentum in the range $q^2 < 0.3$ GeV^2. The nice coincidence of the data for various lattice sizes (except the points refering to the asymmetric lattice) makes it hard to see how finite-volume effects can be blamed for the disagreement with the DS continuum result Eq. (1).

One can ask, whether the ghost-gluon vertex renormalization function $Z_1(q^2)$ is really constant at lower momenta. A recent investigation of this function defined at vanishing gluon momentum for the $SU(2)$ case[10] supports that $Z_1(q^2) \approx 1$ at least for momenta larger than 1 GeV. We have performed an analogous study for $Z_1(q^2)$ in the case of $SU(3)$ gluodynamics. Our results are presented on the right hand side of Fig. 3. There is a slight variation visible in the interval 0.3 GeV$^2 \leq q^2 \leq 5$ GeV^2. But this weak deviation from being constant will not have a dramatic influence on the running coupling. There is a data point at the lowest available momentum derived from the asymmetric lattice which deviates in the opposite direction. Current simulations on larger lattices will enable us to draw conclusions in the near future.

4 Full QCD results

Now let us turn to the full QCD case. We have investigated ILDG gauge field configurations generated in simulations by the QCDSF collaboration[34,35]. $N_f = 2$ flavours of dynamical clover-improved Wilson fermions together with the Wilson plaquette gauge action have been used. The (asymmetric) lattice size is $24^3 \times 48$ possibly demanding some caution in the very infrared as discussed already in the quenched case. The values

Table 1: The parameter values β, κ etc. used for our investigation.

β	κ	κ_c	ma	$a[\mathrm{GeV}^{-1}]$	# conf
5.29	0.13550	0.136410 (09)	0.0246	2.197	60
5.29	0.13590	0.136410 (09)	0.0138	2.324	55
5.25	0.13575	0.136250 (07)	0.0135	2.183	60

of the bare coupling β and of the quark mass ma

$$ma = \frac{1}{2}\left(\frac{1}{\kappa} - \frac{1}{\kappa_c}\right) \tag{10}$$

taken into account are collected in Table 1. The values for κ_c can be found in[35]. The last column of the Table gives the number of configurations investigated. The lattice spacing has been translated into physical units via the Sommer scale r_0/a as determined in[35] with $r_0 = 0.5$ fm. For fixing to Landau gauge we have employed the over-relaxation or the Fourier-accelerated gauge-fixing method. Again we concentrate on `fc` copy results postponing the question of the influence of Gribov copies in the full QCD case to a future publication.

In Fig. 4 we present our full QCD results for the ghost and gluon dressing functions and, for comparison, selected data points of the quenched case (i.e. for infinite quark mass) for $\beta = 6.0$ and a 32^4 lattice. All dressing functions have been renormalized such that $Z_{G,D} = 1$ at $q = 4$ GeV.

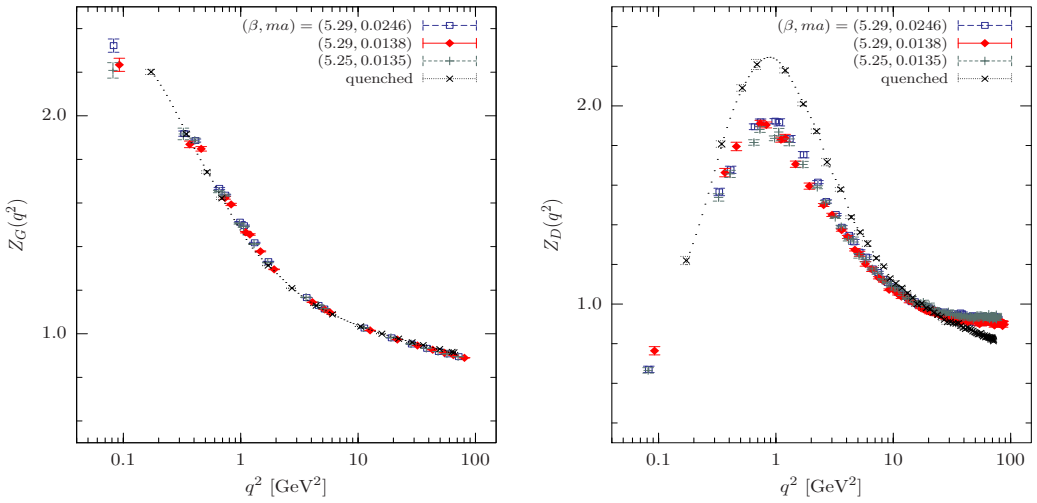

Figure 4: The dressing functions of the ghost propagator Z_G (l.h.s.) and the gluon propagator Z_D (r.h.s.) versus q^2 for full QCD with $N_f = 2$ flavours of clover-improved Wilson fermions (lattice size $24^3 \times 48$). Quenched QCD data for $\beta = 6.0$ and 32^4 are shown for comparison. The dressing functions are renormalized to $Z = 1$ at $q = 4$ GeV. All the data refer to `fc` gauge copies.

The unquenching effect becomes clearly visible for the gluon propagator, whereas the ghost propagator does not show any quark mass dependence. The non-perturbative peak

of the gluon propagator at $q \simeq 1$ GeV becomes softer as the quark mass is decreasing. This has been observed also in recent lattice computations of the gluon propagator using dynamical AsqTad improved staggered quarks[36] as well as from unqenching studies for the ghost and gluon propagators within the DS equation approach[37,38,39]. We refer also to recent lattice studies with dynamical Kogut-Susskind and Wilson fermions[40,41].

In Fig. 5 we show the corresponding MOM scheme running coupling $\alpha_s(q^2)$ and the inverse of the renormalization function $Z_1(q^2)$ of the ghost-gluon vertex as functions of the physical momentum. Again we compare results for full QCD with those for the quenched case at $\beta = 6.0$ on a 32^4 lattice. The normalization factors of the running couplings were determined by fitting the data to the (massless) 2-loop coupling formulae for $\alpha_s(q^2)$ with $N_f = 2$ and $N_f = 0$, respectively, both in the range $q^2 > 30$ GeV^2. The vertex renormalization function was normalized to $Z_1 = 1$ at $q = 4$ GeV for each data set (β, ma) separately.

For the running coupling we observe a quite clear unquenching effect extending from the perturbative range down to the infrared region. Again we see the coupling to turn down in the infrared limit. However, the data points at $q^2 \simeq 0.1$GeV^2 have to be checked carefully on symmetric and larger lattices. The same holds for Z_1.

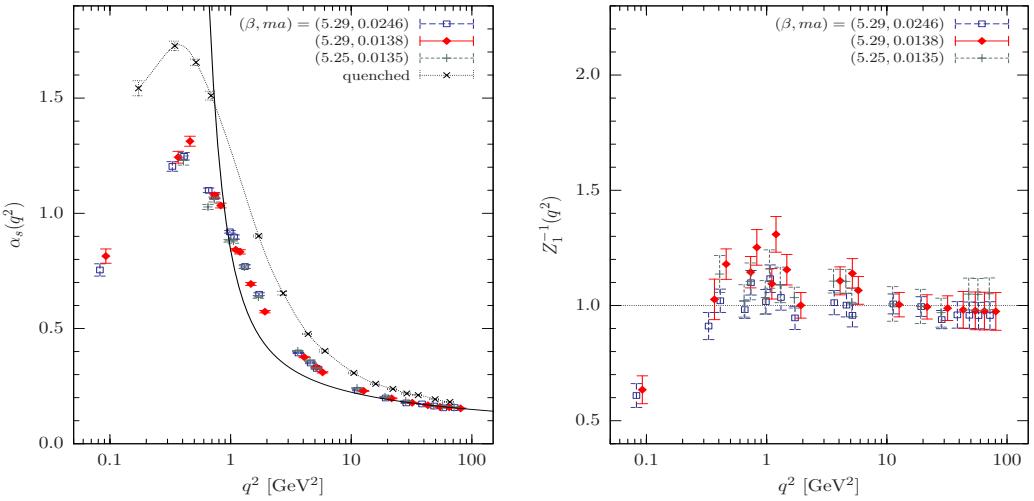

Figure 5: The running coupling (l.h.s.) and the inverse renormalization function Z_1^{-1} of the ghost-gluon vertex (r.h.s.) are shown as functions of the physical momentum for full QCD. For comparison, the quenched QCD running coupling data for $\beta = 6.0,\ 32^4$ are shown with a spline fit line to guide the eye. The 2-loop fit to $\alpha_s(q^2)$ for $N_f = 2$ is drawn with the solid line. The vertex renormalization function is normalized to $Z_1 = 1$ at $q = 4$ GeV.

5 Conclusions

We have studied the low-momentum region of QCD within the Landau gauge using Monte Carlo simulations with the Wilson plaquette action and various lattice sizes from 16^4 to 32^4 for the quenched case in the range of bare couplings $\beta = 5.8, \ldots, 6.2$. In this way we have reached momenta down to $q^2 \simeq 0.1$GeV^2. Moreover, for studying

unquenching effects we have carried out an analogous investigation in full QCD for the case of two improved Wilson flavours for a couple of quark mass values but only one lattice size $24^3 \times 48$. Our data presented here refer to first gauge copies as obtained from over-relaxation or Fourier-accelerated gauge fixing. In the quenched QCD case we have seen clear Gribov copy effects in the infrared region for the ghost propagator. The ghost propagator becomes less singular within a $O(5\%)$ deviation, when better gauge copies are taken. We have found indications that the Gribov effect also weakens as the volume is increasing. Towards $q \to 0$ in the infrared momentum region, the gluon dressing functions in quenched as well as full QCD were shown to decrease, while the ghost dressing functions turned out to rise. However, the connected power laws predicted by the infinite-volume DS approach could not be confirmed on the basis of our data. Correspondingly, the behaviour of the running coupling $\alpha_s(q^2)$ in a suitable momentum subtraction scheme (based on the ghost-gluon vertex) does not approach the expected finite limit. Instead, this coupling has been found to decrease for lower momenta after passing a turnover at $q^2 \approx 0.4$ GeV^2 for quenched ($N_f = 0$) as well as for full QCD ($N_f = 2$). Unquenching effects have been clearly recovered for the gluon propagator, whereas the ghost propagator was almost unchanged. This is in one-to-one correspondence with what has been recently found in the Dyson-Schwinger equation approach. However, the puzzle of the existence of a non-trivial infrared fixed point in the infinite volume limit remains unsolved.

Acknowledgements

All simulations have been done on the IBM pSeries 690 at HLRN. We are indebted to the QCDSF collaboration for providing us with their gauge field configurations via the International Lattice DataGrid (ILDG) (`http://www.lqcd.org/ildg/`). We used *ltools* for getting those configurations[42]. We thank Dirk Pleiter and Stefan Wollny for their help as well as H. Stüben for contributing parts of the program code. We also acknowledge discussions with G. Burgio, C. Fischer and V.K. Mitrjushkin. This work has been supported by the DFG under contract FOR 465 (Forschergruppe *Lattice Hadron Phenomenology*). A. Sternbeck acknowledges support of the DFG-funded graduate school GK 271.

References

1. D. Zwanziger, *Nucl. Phys.* B **412**, 657 (1994).
2. V. N. Gribov, *Nucl. Phys.* B **139**, 1 (1978).
3. T. Kugo and I. Ojima, *Prog. Theor. Phys. Suppl.* **66**, 1 (1979).
4. L. von Smekal, R. Alkofer, and A. Hauck, *Phys. Rev. Lett.* **79**, 3591 (1997).
5. L. von Smekal, A. Hauck, and R. Alkofer, *Ann. Phys.* **267**, 1 (1998).
6. R. Alkofer and L. von Smekal, *Phys. Rept.* **353**, 281 (2001).
7. D. Zwanziger, *Phys. Rev.* D **65**, 094039 (2002).
8. C. Lerche and L. von Smekal, *Phys. Rev.* D **65**, 125006 (2002).
9. J. C. Taylor, *Nucl. Phys.* B **33**, 436 (1971).
10. A. Cucchieri, T. Mendes, and A. Mihara, *JHEP* **12**, 012 (2004).
11. P. Boucaud, J. P. Leroy, J. Micheli, O. Pene, and C. Roiesnel, *JHEP* **10**, 017 (1998).
12. P. Boucaud et al., *JHEP* **04**, 005 (2003).
13. J. Skullerud and A. Kizilersu, *JHEP* **09**, 013 (2002).

14. C. S. Fischer, R. Alkofer, and H. Reinhardt, *Phys. Rev.* D **65**, 094008 (2002).
15. C. S. Fischer, B. Grüter, and R. Alkofer, (2005), hep-ph/0506053.
16. P. Boucaud et al., (2005), hep-ph/0507104.
17. W. Schleifenbaum, A. Maas, J. Wambach, and R. Alkofer, *Phys. Rev.* D **72**, 014017 (2005).
18. R. Alkofer, C. S. Fischer, and F. J. Llanes-Estrada, *Phys. Lett.* B **611**, 279 (2005).
19. J. C. R. Bloch, A. Cucchieri, K. Langfeld, and T. Mendes, *Nucl. Phys.* B **687**, 76 (2004).
20. H. Suman and K. Schilling, *Phys. Lett.* B **373**, 314 (1996).
21. S. Furui and H. Nakajima, *Phys. Rev.* D **69**, 074505 (2004).
22. S. Furui and H. Nakajima, *Phys. Rev.* D **70**, 094504 (2004).
23. A. Sternbeck, E.-M. Ilgenfritz, M. Müller-Preussker, and A. Schiller, *Phys. Rev.* D **72**, 014507 (2005).
24. A. Sternbeck, E.-M. Ilgenfritz, and M. Müller-Preussker, *Phys. Rev.* D in print (2005), hep-lat/0510109.
25. A. Sternbeck, E.-M. Ilgenfritz, M. Müller-Preussker, and A. Schiller, *PoS* **LAT2005**, 333 (2005).
26. I. L. Bogolubsky, G. Burgio, V. K. Mitrjushkin, and M. Müller-Preussker, *Phys. Rev.* D submitted (2005), hep-lat/0511056.
27. T. D. Bakeev, E.-M. Ilgenfritz, V. K. Mitrjushkin, and M. Müller-Preussker, *Phys. Rev.* D **69**, 074507 (2004).
28. D. B. Leinweber, J. I. Skullerud, A. G. Williams, and C. Parrinello, *Phys. Rev.* D **60**, 094507 (1999.
29. S. Necco and R. Sommer, *Nucl. Phys.* B **622**, 328 (2002).
30. A. Cucchieri, *Nucl. Phys.* B **508**, 353 (1997).
31. D. Zwanziger, *Phys. Rev.* D **69**, 016002 (2004).
32. P. J. Silva and O. Oliveira, *Nucl. Phys.* B **690**, 177 (2004).
33. O. Oliveira and P. J. Silva, *AIP Conf. Proc.* **756**, 290 (2005).
34. M. Göckeler et al., (2004), hep-ph/0409312.
35. M. Göckeler et al., (2005), hep-ph/0502212.
36. P. O. Bowman, U. M. Heller, D. B. Leinweber, M. B. Parappilly, and A. G. Williams, *Phys. Rev.* D **70**, 034509 (2004).
37. C. S. Fischer, R. Alkofer, W. Cassing, F. Llanes-Estrada, and P. Watson, (2005), hep-ph/0511147.
38. C. S. Fischer, P. Watson, and W. Cassing, *Phys. Rev.* D **72**, 094025 (2005).
39. C. S. Fischer and R. Alkofer, *Phys. Rev.* D **67**, 094020 (2003).
40. S. Furui and H. Nakajima, (2005), hep-lat/0503029.
41. S. Furui and H. Nakajima, *PoS* **LAT2005**, 291 (2005).
42. H. Stüben and S. Wollny, (2005), hep-lat/0512008.